

AD-A281 458

BEST AVAILABLE COPY

CMR TR 692  
CMR TR 3172

DAAH-0493G0419  
November 1993

ESTIMATION OF VEHICLE DYNAMICS  
FROM MONOCULAR NOISY IMAGES

Yi Sheng Yao  
Rama Chellappa\*

Department of Electrical Engineering and  
Center for Automation Research and  
\*Institute for Advanced Computer Studies  
University of Maryland  
College Park, MD 20742-3275

COMPUTER VISION LABORATORY



CENTER FOR AUTOMATION RESEARCH

UNIVERSITY OF MARYLAND  
COLLEGE PARK, MARYLAND  
20742-3275

94-21215

CAR-TR-692  
CS-TR-3172

DAAH-0493G0419  
November 1993

**ESTIMATION OF VEHICLE DYNAMICS  
FROM MONOCULAR NOISY IMAGES**

Yi-Sheng Yao  
Rama Chellappa\*

Department of Electrical Engineering and  
Center for Automation Research and  
\*Institute for Advanced Computer Studies  
University of Maryland  
College Park, MD 20742-3275

**Abstract**

This paper presents a new model-based egomotion estimation algorithm for an autonomous vehicle navigating through rough terrain. Due to the uneven terrain, the vehicle undergoes bouncing, pitch and roll motion. To reliably accomplish other tasks such as tracking and obstacle avoidance using visual inputs, it is essential to consider these disturbances. In this paper, two vehicle models available in the literature are used for egomotion estimation. The Half Vehicle Model (HVM) takes into account the bouncing and pitch motion of the vehicle, and the Full Vehicle Model (FVM) also considers the roll motion. The dynamics of the vehicle are formulated using standard equations of motion. Assuming that depth information is known for some landmarks in the scene (e.g., obtained from a laser range finder), a feature-based approach is proposed to estimate vehicle motion parameters such as the vertical movement of the center of mass and the instantaneous angular velocity. An Iterated Extended Kalman Filter (IEKF) is used for recursive parameter estimation. Simulation results for both known and unknown terrain are presented.

## 1 Introduction

There has been growing interest among computer vision researchers in solving the problem of navigating an autonomous vehicle through uneven terrain. The knowledge of the vehicle's pose and motion relative to some reference system is a prerequisite for the success of other navigation tasks such as object recognition and obstacle avoidance. Although the Inertial Navigation System (INS) on board the vehicle provides accurate motion information over short periods, there are problems over long periods due to sensor drift. An independent estimate of the vehicle's motion can be combined with INS information to provide more reliable information.

In recent years, the wealth of information contained in long sequences of images has attracted the attention of computer vision researchers [3, 14, 15, 16]. Motion estimation based on two or three frames has been shown to be very sensitive to noise [1, 2, 7, 10], leading to an increasing interest in long sequence based methods. Due to lack of knowledge of the forces and torques that result in movements of the camera, most model-based motion estimation algorithms assume a smooth trajectory over time in order to exploit temporal information [3, 14, 15, 16]. For a vehicle traversing uneven terrain, the camera undergoes nonsmooth motion. Thus the performance of these algorithms may degrade, depending on the roughness of the terrain, the vehicle speed, etc.

In order to describe the motion of the vehicle, both its lateral dynamics (or kinematics) and its suspension dynamics should be considered [13], in connection with direction control and stabilization behavior, respectively. The work in [5] focuses on the use of lateral vehicle dynamics in 3-D road tracking. In this paper, we develop a motion estimation algorithm mainly from the suspension dynamics point of view and use simple assumptions about lateral kinematics. Two vehicle models, which can be found in the literature on optimal design of suspension systems [4, 8], are used in our work: A Half Vehicle Model (HVM), consisting of two wheels, which takes into account vehicle bouncing and pitch motion in rough terrain; and a Full Vehicle Model (FVM), which considers the correlation between the left and right tracks, in order to include roll motion in addition to bouncing and pitch motion. Both models assume that each tire always contacts the surface at a point, tire stiffness is modeled by a linear spring, and the suspension system is modeled by putting a linear spring and a damper at each corner of the vehicle body. Assuming that the vehicle follows a straight path with constant speed along the longitudinal axis (i.e. there is no steering control), the motion of the vehicle can be described using standard equations of motion. A camera is assumed to be rigidly attached to the vehicle body with known orientation relative to a coordinate system

attached to the vehicle. The 3-D coordinates of some landmarks relative to a fixed reference system are also assumed to be available; these can be obtained, for example, by a vehicle-mounted laser range finder. Then, given the image coordinates of these feature points at different time instants, an IEKF [11] is used to recursively estimate the motion parameters of the vehicle.

The organization of this paper is as follows. Section 2 gives detailed descriptions of the two vehicle models and the physical laws governing the motion of unsprung and sprung masses. The recursive filter formulation of the algorithm is given in Section 3. Section 4 presents simulation results, and conclusions are presented in Section 5.

## 2 Suspension dynamics

We describe the vehicle models and their behaviors under various surface inputs. In both models, an inertial coordinate system  $I$  is fixed on the ground. A vehicle coordinate system  $V$  moves with the vehicle with its origin at the vehicle's center of mass and its axes coinciding with the principal axes of the vehicle's body. When there is no confusion, the time dependence of all quantities will be suppressed in the following derivations.

### 2.1 The half vehicle model (HVM)

A two-wheel vehicle model is shown in Fig. 1. It represents the bouncing and pitch motions of the vehicle body, which result from different surface inputs to the front and rear wheels.  $M_{wf}$  and  $M_{wr}$  represent the unsprung masses of the front and rear wheels and their axles. Each tire is modeled by a linear spring with stiffness coefficient  $K_T$ .  $K_f, C_f, K_r$  and  $C_r$  are the characteristics of the linear springs and dampers that model the suspension system.

Assuming that the pitch motion is small, so that

$$\sin \theta \approx \theta$$

holds, and that the variations of the springs and dampers are along the vertical direction, the motion of the vehicle body can be described as follows [4]:

$$\begin{aligned} M_{wf}\ddot{x}_1 &= K_f d_2 + C_f \dot{d}_2 - K_T d_1 \\ M_{wr}\ddot{x}_2 &= K_r d_4 + C_r \dot{d}_4 - K_T d_3 \\ M_B\ddot{X} &= -(K_f d_2 + C_f \dot{d}_2) - (K_r d_4 + C_r \dot{d}_4) \\ I\ddot{\theta} &= -(K_f d_2 + C_f \dot{d}_2)W_A + (K_r d_4 + C_r \dot{d}_4)W_B \end{aligned} \tag{1}$$

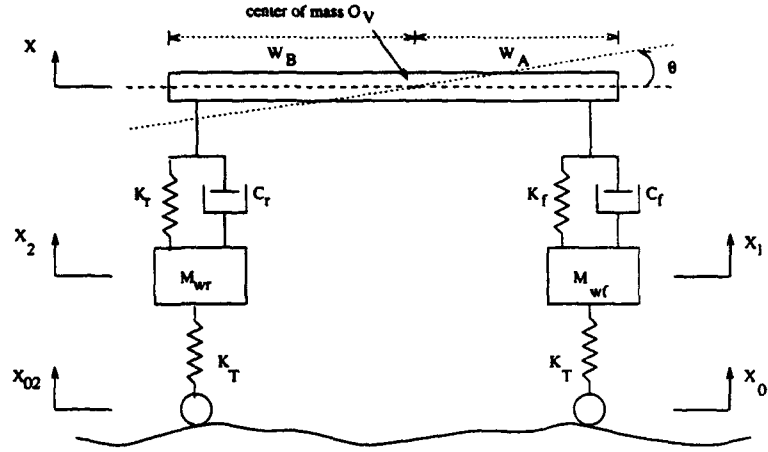


Figure 1: The half vehicle model [4].

where  $X$  is the displacement of the center of mass of the vehicle,  $\theta$  is the pitch angle, and  $I$  represents the moment of inertia with respect to the pitch axis, which is normal to the half-vehicle plane. The displacements of the connection points  $\{d_i, i = 1, \dots, 4\}$  are approximated by

$$\begin{aligned} d_1 &= x_1 - x_{01} \\ d_2 &= X + W_A \theta - x_1 \\ d_3 &= x_2 - x_{02} \\ d_4 &= X - W_B \theta - x_2 \end{aligned} \quad (2)$$

where  $x_{01}, x_{02}$  are the surface excitation inputs to the front and rear wheels, respectively.

## 2.2 The full vehicle model (FVM)

A four-wheel vehicle model is shown in Fig. 2. For a vehicle following a straight path, in addition to bouncing and pitching behavior, rolling due to the different inputs to left and right wheels is considered in this model. As in the HVM, the tires are modeled by linear springs, and linear springs and dampers are used to model the suspension system.

### Wheel Motion

For simplicity, we refer the heights of the four wheels and the four corners of the vehicle body above the flat ground when the vehicle is at rest (i.e. when gravity is the only external force acting on the vehicle) as reference heights. Let  $\{x_1, x_3, x_5, x_7\}$  be the unsprung mass displacements,  $\{x_2, x_4, x_6, x_8\}$  be the displacements of the four corners, and  $\{x_{0i}, i = 1, \dots, 4\}$  be road excitation

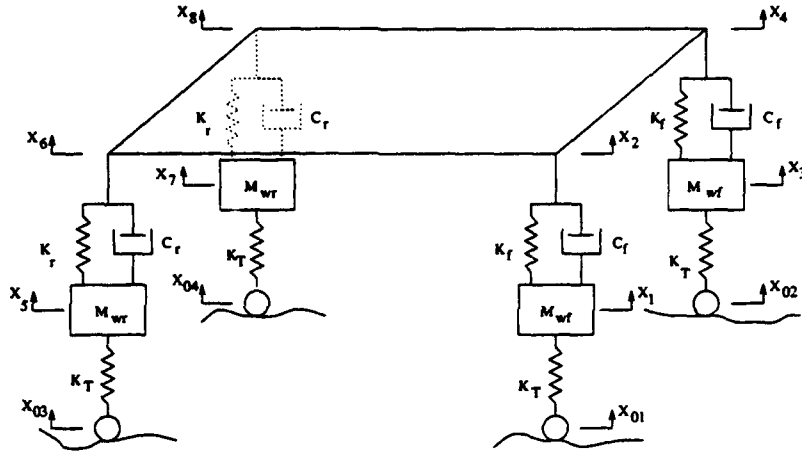


Figure 2: The full vehicle model [8].

inputs. All these quantities are measured with respect to their own reference heights, as shown in Fig. 2. Assuming that the linear springs and dampers in the model are restricted to move only vertically, the displacements between the different connection points are

$$\begin{aligned}
 d_1 &= x_1 - x_{01}, & d_2 &= x_2 - x_1 \\
 d_3 &= x_3 - x_{02}, & d_4 &= x_4 - x_3 \\
 d_5 &= x_5 - x_{03}, & d_6 &= x_6 - x_5 \\
 d_7 &= x_7 - x_{04}, & d_8 &= x_8 - x_7
 \end{aligned} \tag{3}$$

and the motion of the unsprung masses is described by Newton's law as

$$\begin{aligned}
 M_{wf}\ddot{x}_1 &= K_f d_2 + C_f \dot{d}_2 - K_T d_1 \\
 M_{wf}\ddot{x}_3 &= K_f d_4 + C_f \dot{d}_4 - K_T d_3 \\
 M_{wr}\ddot{x}_5 &= K_r d_6 + C_r \dot{d}_6 - K_T d_5 \\
 M_{wr}\ddot{x}_7 &= K_r d_8 + C_r \dot{d}_8 - K_T d_7
 \end{aligned} \tag{4}$$

### Bouncing

In Fig. 3, let  $\{\vec{i}, \vec{j}, \vec{k}\}$  and  $\{\vec{i}', \vec{j}', \vec{k}'\}$  be the axes of the coordinate systems  $I$  and  $V$  respectively. Here again, the suspension forces  $\{\vec{F}_i, i = 1, \dots, 4\}$  which act on the four corners are always in the  $\vec{i}$ -direction, i.e.

$$\begin{aligned}
 \vec{F}_1 &= -(K_f d_2 + C_f \dot{d}_2)\vec{i} = F_1 \vec{i} \\
 \vec{F}_2 &= -(K_f d_4 + C_f \dot{d}_4)\vec{i} = F_2 \vec{i} \\
 \vec{F}_3 &= -(K_r d_6 + C_r \dot{d}_6)\vec{i} = F_3 \vec{i} \\
 \vec{F}_4 &= -(K_r d_8 + C_r \dot{d}_8)\vec{i} = F_4 \vec{i}
 \end{aligned} \tag{5}$$

Vehicle bouncing is thus restricted to the  $\vec{i}$ -direction and is described by

$$M_B \ddot{X} = \sum_{i=1}^4 F_i \quad (6)$$

where  $M_B$  is the mass of the vehicle's body and  $X$  is the displacement of its center of mass.

### Pitch and Roll Motions

As shown in Fig. 3, the four suspension forces which act on the four corners at the same time result in change of the vehicle's angular momentum. In order to describe the pitch and roll motion of the vehicle's body, we need to find its orientation with respect to the inertial coordinate system—in other words, we need to find the rotation matrix which aligns  $V$  with  $I$ . There are many ways to represent this rotation matrix [9]. Since the instantaneous angular velocity changes with time, we use a quaternion representation. In the following, a vector  $P$  is denoted by  $P_I$  if its components are represented in  $I$ , and by  $P_V$  if they are represented in  $V$ .

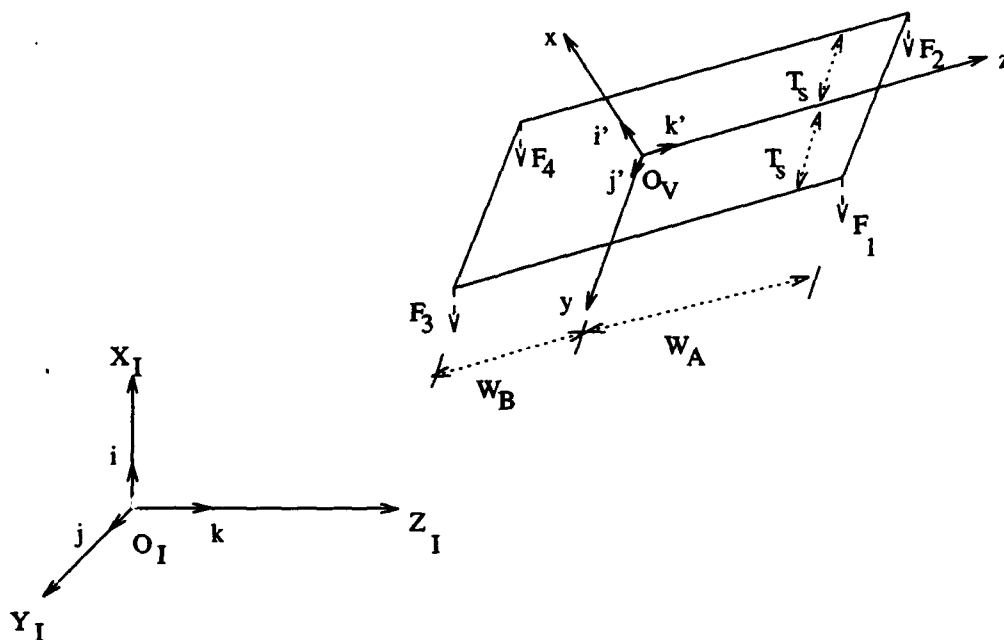


Figure 3: The inertial coordinate system  $I$  and the vehicle coordinate system  $V$ .

Let  $\underline{w}_V = (w_x, w_y, w_z)^T$  be the instantaneous angular velocity of the vehicle's body with respect to the vehicle coordinate system  $V$ . By choosing the axes of  $V$  to coincide with the principal axes of the vehicle's body, Euler's equations of motion [12] can be applied to find the instantaneous

angular velocity:

$$\begin{pmatrix} M_x \\ M_y \\ M_z \end{pmatrix} = \begin{pmatrix} I_{xx}\dot{w}_x + w_y w_z (I_{zz} - I_{yy}) \\ I_{yy}\dot{w}_y + w_z w_x (I_{xx} - I_{zz}) \\ I_{zz}\dot{w}_z + w_x w_y (I_{yy} - I_{xx}) \end{pmatrix} \quad (7)$$

where  $\{I_{xx}, I_{yy}, I_{zz}\}$  are the moments of inertia of the vehicle with respect to the coordinate axes of  $V$  (these are constants, because  $V$  moves with the vehicle's body) and  $(M_x, M_y, M_z)^T$  is the net torque applied by the suspension forces, with its components expressed in  $V$ .

The instantaneous angular velocity and the rotation matrix are related through the quaternions as follows: Let the quaternions  $\underline{q}$  be represented by

$$\underline{q} = (q_1, q_2, q_3, q_4)^T$$

Then the dependence of  $\underline{q}$  on  $\underline{\omega}$  is [16]

$$\dot{\underline{q}} = \Omega[\underline{\omega}] \underline{q} \quad (8)$$

where

$$\Omega[\underline{\omega}] = \frac{1}{2} \begin{pmatrix} 0 & -w_Z & w_Y & -w_X \\ w_Z & 0 & -w_X & -w_Y \\ -w_Y & w_X & 0 & -w_Z \\ w_X & w_Y & w_Z & 0 \end{pmatrix} \quad (9)$$

and  $(w_X, w_Y, w_Z)^T$  are the components of the instantaneous angular velocity represented in  $I$ . The rotation matrix can then be obtained as follows:

$$\begin{aligned} R[\underline{q}] &= \begin{pmatrix} q_1^2 - q_2^2 - q_3^2 + q_4^2 & 2(q_1 q_2 + q_3 q_4) & 2(q_1 q_3 - q_2 q_4) \\ 2(q_1 q_2 - q_3 q_4) & -q_1^2 + q_2^2 - q_3^2 + q_4^2 & 2(q_2 q_3 + q_1 q_4) \\ 2(q_1 q_3 + q_2 q_4) & 2(q_2 q_3 - q_1 q_4) & -q_1^2 - q_2^2 + q_3^2 + q_4^2 \end{pmatrix} \\ &\equiv \begin{pmatrix} r_1 & r_2 & r_3 \\ r_4 & r_5 & r_6 \\ r_7 & r_8 & r_9 \end{pmatrix} \end{aligned} \quad (10)$$

When the rotation matrix (10) is available, the relative orientation of  $I$  and  $V$  is known. The coordinates of a vector  $P$  in the two systems are now related through the rotation matrix, i.e.

$$R[\underline{q}] P_V = P_I \quad (11)$$



### 3 Recursive filter formulation

Unlike batch estimators, which process all the data, recursive filters update their estimates of the parameters as new information becomes available. Among recursive estimators, EKF and IEKF are both suitable for estimating the parameters of a nonlinear system. The measurement equations in HVM and FVM are similar; we will therefore describe only the corresponding plant equations.

#### 3.1 The plant equations

##### HVM

Let

$$\underline{x} \equiv (x_1, \dot{x}_1, x_2, \dot{x}_2, X, \dot{X}, \theta, \dot{\theta}, v)^T$$

be the state vector, where  $v$  is the vehicle speed along the longitudinal axis, expressed in system  $I$ . The plant equation is obtained from (1) and (2) as

$$\dot{\underline{x}} = A \underline{x} + B \underline{x}_0 \quad (12)$$

where

$$A = \begin{pmatrix} 0 & 1 & 0 & 0 & 0 & 0 & 0 & 0 & 0 \\ \frac{-(K_f + K_T)}{M_{wf}} & \frac{-C_f}{M_{wf}} & 0 & 0 & \frac{K_f}{M_{wf}} & \frac{C_f}{M_{wf}} & \frac{K_f W_A}{M_{wf}} & \frac{C_f W_A}{M_{wf}} & 0 \\ 0 & 0 & 0 & 1 & 0 & 0 & 0 & 0 & 0 \\ 0 & 0 & \frac{-(K_r + K_T)}{M_{wr}} & \frac{-C_r}{M_{wr}} & \frac{K_r}{M_{wr}} & \frac{C_r}{M_{wr}} & \frac{-K_r W_B}{M_{wr}} & \frac{-C_r W_B}{M_{wr}} & 0 \\ 0 & 0 & 0 & 0 & 0 & 1 & 0 & 0 & 0 \\ \frac{K_f}{M_B} & \frac{C_f}{M_B} & \frac{K_r}{M_B} & \frac{C_r}{M_B} & \frac{-(K_f + K_r)}{M_B} & \frac{-(C_f + C_r)}{M_B} & \frac{-(K_f W_A - K_r W_B)}{M_B} & \frac{-(C_f W_A - C_r W_B)}{M_B} & 0 \\ 0 & 0 & 0 & 0 & 0 & 0 & 0 & 1 & 0 \\ \frac{K_f W_A}{I} & \frac{C_f W_A}{I} & \frac{-K_r W_B}{I} & \frac{-C_r W_B}{I} & \frac{(-K_f W_A + K_r W_B)}{I} & \frac{(-C_f W_A + C_r W_B)}{I} & \frac{-(K_f W_A^2 + K_r W_B^2)}{I} & \frac{-(C_f W_A^2 + C_r W_B^2)}{I} & 0 \\ 0 & 0 & 0 & 0 & 0 & 0 & 0 & 0 & 1 \end{pmatrix}$$

and

$$B = \begin{pmatrix} 0 & \frac{K_T}{M_{wf}} & 0 & 0 & 0 & 0 & 0 & 0 & 0 \\ 0 & 0 & 0 & \frac{K_T}{M_{wr}} & 0 & 0 & 0 & 0 & 0 \end{pmatrix}^T \quad \underline{x}_0 = \begin{pmatrix} x_{01} & x_{02} \end{pmatrix}^T$$

where the forward speed is assumed to be constant.

##### FVM

Again, let

$$\underline{x} \equiv (x_1, \dot{x}_1, x_3, \dot{x}_3, x_5, \dot{x}_5, x_7, \dot{x}_7, X, \dot{X}, \underline{\omega}_f^T, \underline{q}^T, v)^T$$

be the state vector, where  $v$  is the vehicle's forward speed, represented in  $I$ . Note that for convenience, the angular velocity is expressed in  $I$ . Assuming that the vehicle moves along a straight path on the horizontal plane with constant speed, the plant equation is obtained from (4), (6), (7) and (8) as

$$\dot{\underline{x}} = f(\underline{x}, \underline{x}_0) \quad (13)$$

where

$$f(\underline{x}, \underline{x}_0) = \begin{pmatrix} \dot{x}_1 \\ \frac{1}{M_{wf}}(K_f d_2 + C_f \dot{d}_2 - K_T d_1) \\ \dot{x}_3 \\ \frac{1}{M_{wf}}(K_f d_4 + C_f \dot{d}_4 - K_T d_3) \\ \dot{x}_5 \\ \frac{1}{M_{wr}}(K_r d_6 + C_r \dot{d}_6 - K_T d_5) \\ \dot{x}_7 \\ \frac{1}{M_{wr}}(K_r d_8 + C_r \dot{d}_8 - K_T d_7) \\ \dot{x} \\ \frac{1}{M_B}(F_1 + F_2 + F_3 + F_4) \\ R(\underline{q}) \begin{bmatrix} \frac{1}{I_{xx}}(M_x - \omega_y \omega_z (I_{zz} - I_{yy})) \\ \frac{1}{I_{yy}}(M_y - \omega_z \omega_x (I_{xx} - I_{zz})) \\ \frac{1}{I_{zz}}(M_z - \omega_x \omega_y (I_{yy} - I_{xx})) \end{bmatrix} \\ \frac{1}{2} \begin{pmatrix} 0 & -\omega_Z & \omega_Y & -\omega_X \\ \omega_Z & 0 & -\omega_X & -\omega_Y \\ -\omega_Y & \omega_X & 0 & -\omega_Z \\ \omega_X & \omega_Y & \omega_Z & 0 \end{pmatrix} \underline{q} \\ 0 \end{pmatrix} \quad (14)$$

Assuming that the movements of the linear springs and shock absorbers in the  $\vec{j}$  and  $\vec{k}$ -directions are negligible compared to their movements in the  $\vec{i}$ -direction,  $d_2, d_4, d_6$  and  $d_8$  are approximated by

$$\begin{aligned} d_2 &= X - x_1 + r_2 T_s + r_3 W_A \\ d_4 &= X - x_3 - r_2 T_s + r_3 W_A \\ d_6 &= X - x_5 + r_2 T_s - r_3 W_B \\ d_8 &= X - x_7 - r_2 T_s - r_3 W_B \end{aligned} \quad (15)$$

where  $r_2, r_3$  are the elements of the rotation matrix (10), and  $T_s, W_A$  and  $W_B$  are the dimensions of the vehicle's body, as shown in Fig. 3.

In the above formulation,  $\underline{\omega}_I$  is used to represent the angular velocity in the state vector in order to preserve the dynamics of the quaternions (8). To include Euler's equations of motion in the plant equation, the dynamics of the angular velocity  $\underline{\omega}$  should be expressed in the inertial coordinate system  $I$ . The representation of  $\underline{\omega}$  in the  $V$  coordinate system can be found from (11):

$$\underline{\omega}_V = R^T[q] \underline{\omega}_I \quad (16)$$

Because of the characteristics of the angular velocity [12], it follows that

$$\begin{pmatrix} \dot{\omega}_x \\ \dot{\omega}_y \\ \dot{\omega}_z \end{pmatrix} = R^T[q] \dot{\underline{\omega}}_I \quad (17)$$

where  $\dot{\underline{\omega}}_I$  is the rate of change of the angular velocity with components represented in system  $I$ . Finally, the relationship between  $(M_x, M_y, M_z)^T$  and  $\underline{x}$  is derived in Appendix A.

As shown above, to describe roll motion in addition to the bouncing and pitch motions, the linear plant equation of HVM is replaced by a nonlinear equation in FVM.

### 3.2 The measurement equations

Consider the camera coordinate system and the imaging model shown in Fig. 4. Let  $P_I^j = (X^j, Y^j, Z^j)^T$  be the coordinates of the  $j^{\text{th}}$  feature point, let  $O_V(t) = (X(t) + h, 0, vt)^T$  be the coordinates of the vehicle's center of mass at time  $t$  (both in  $I$ ), and let  $h$  be the reference height of the center of mass. Assuming that the camera is fixed with respect to the vehicle system  $V$ , i.e. its projection center  $O_C(t)$  in  $V$  is  $(d_0, 0, l)^T$ , then  $P_C^j(t) = (x^j(t), y^j(t), z^j(t))^T$ , the coordinates of the  $j^{\text{th}}$  feature point in the camera coordinate system  $C$ , are

$$\begin{pmatrix} x^j(t) \\ y^j(t) \\ z^j(t) \end{pmatrix} = R_0 \left\{ R^T(q) \left\{ \begin{pmatrix} X^j \\ Y^j \\ Z^j \end{pmatrix} - \begin{pmatrix} X(t) + h \\ 0 \\ vt \end{pmatrix} \right\} - \begin{pmatrix} d_0 \\ 0 \\ l \end{pmatrix} \right\} \quad (18)$$

where  $R_0$  aligns the camera coordinate system  $C$  with the vehicle coordinate system  $V$ . For simplicity,  $R_0$  is set equal to the identity matrix in our discussion.

The image plane coordinates of the  $j^{\text{th}}$  feature point at time  $t$ , can now be obtained by applying the perspective projection formula. The resulting measurement equations for the recursive filter

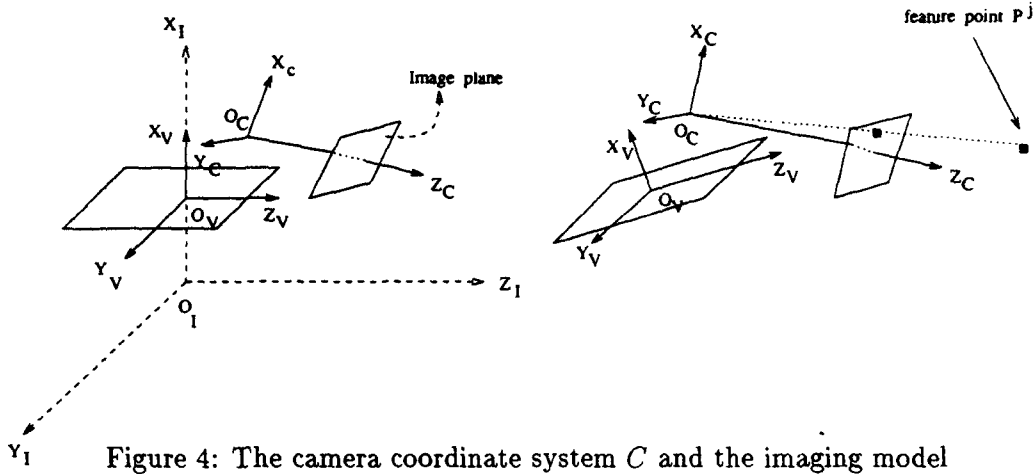


Figure 4: The camera coordinate system  $C$  and the imaging model

are

$$\begin{aligned} X_j(t_i) &= f \frac{R_1^T(P_I^j - O_V(t_i)) - d_0}{R_3^T(P_I^j - O_V(t_i)) - l} + n_{X_j}(t_i) \quad j = 1, \dots, N \\ Y_j(t_i) &= f \frac{R_2^T(P_I^j - O_V(t_i))}{R_3^T(P_I^j - O_V(t_i)) - l} + n_{Y_j}(t_i) \end{aligned} \quad (19)$$

where  $f$  is the focal length and  $N$  is the number of available feature points.  $\{R_i^T, i = 1, 2, 3\}$  is the  $i^{\text{th}}$  row of the rotation matrix  $R^T$  and  $(n_{X_j}(t_i), n_{Y_j}(t_i))$  takes into account measurement noise such as quantization noise. Note that if the HVM is employed, the rotation matrix

$$\begin{pmatrix} \cos(\theta) & 0 & -\sin(\theta) \\ 0 & 1 & 0 \\ \sin(\theta) & 0 & \cos(\theta) \end{pmatrix}$$

should be used for  $R$  in (19), while the quaternion representation of the rotation matrix in (10) should be used for the FVM.

After the plant and measurement equations have been formulated, EKF or IEKF can be applied to estimate the vehicle dynamics.

#### 4 Experimental results

Natural terrain, in general, can be decomposed into low-frequency and high-frequency components; the low-frequency component maintains the road's shape, and the high-frequency component takes into account its micro-roughness. In the following simulation, we generated the micro-roughness from a first order Markov process and superimposed it on designed shapes in order to obtain the surface excitation inputs to the front wheels. Since we assume that the vehicle moves along a

straight path with constant speed, the inputs to the rear wheels are the same as the inputs to the front wheels except for a time delay, i.e.

$$x_{02}(t) = x_{01}(t - L/v) \quad (20)$$

for HVM, and

$$x_{03}(t) = x_{01}(t - L/v) \quad (21)$$

$$x_{04}(t) = x_{02}(t - L/v) \quad (22)$$

for FVM, where  $L$  is the length of the vehicle. Fig. 5 shows the surface inputs used in our simulation. Note that in the case of the FVM, during time interval  $[0, 4.0]$  the excitation inputs to the left and right wheels are the same, so that no roll motion should result. The front left wheel then encounters a bump during the time interval  $[4.0, 7.2]$ , which makes the vehicle start rolling. After the bump, the surfaces are again the same for both the left and right wheels.

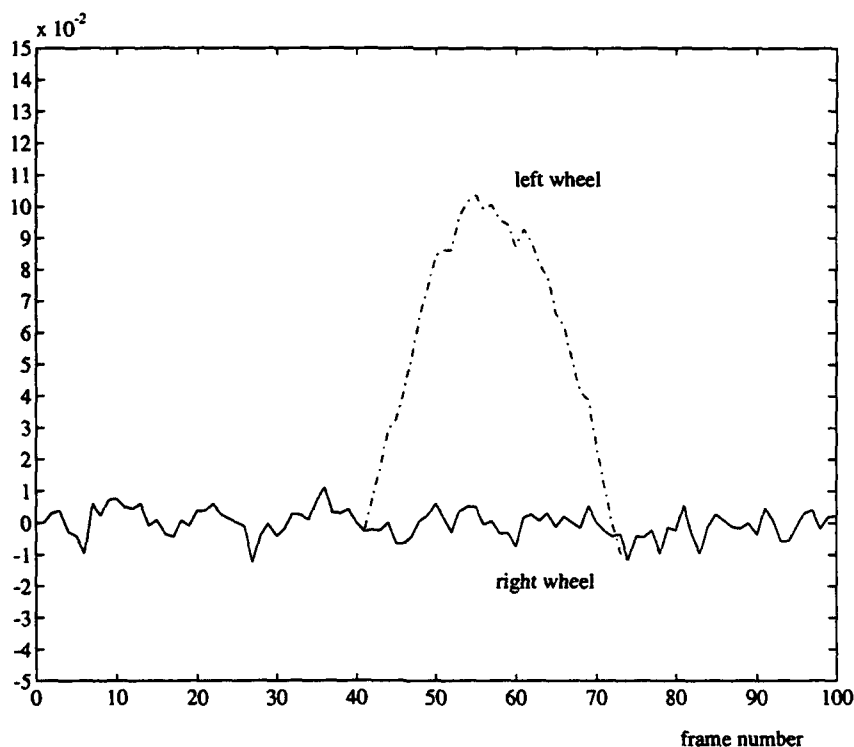


Figure 5: The excitation inputs to the front wheels

The values of the vehicle parameters are listed in Table 1 [8]. For the HVM, the plant equation in (12) is first discretized. The ground truths of the states are then obtained, with the initial

Table 1: Vehicle parameters

$M_B$	1710 kg	$K_T$	200.0 kN/m	$L$	2.69 m
$M_{wf}$	57.5 kg	$K_f$	18.0 kN/m	$W_A$	1.353 m
$M_{wr}$	75 kg	$C_f$	1.0 kN/m/sec	$T_S$	0.595 m
$I_{xx}$	1233.05 kg-m <sup>2</sup>	$K_r$	10.0 kN/m	$d_0$	0.6 m
$I_{yy}$	1031.25 kg-m <sup>2</sup>	$C_r$	1.0 kN/m/sec	$l$	1.35 m
$I_{zz}$	201.79 kg-m <sup>2</sup>			$h$	2.0 m

conditions arbitrarily chosen as

$$(0.1 \quad -0.3 \quad -0.05 \quad 0.4 \quad 0.03 \quad 0.06 \quad 0.01 \quad 0.04 \quad 1.345)^T$$

The resulting bouncing and pitch motions of the vehicle's body are shown in Fig. 6. Note that the left wheel input shown in Fig. 5 is used as the terrain.

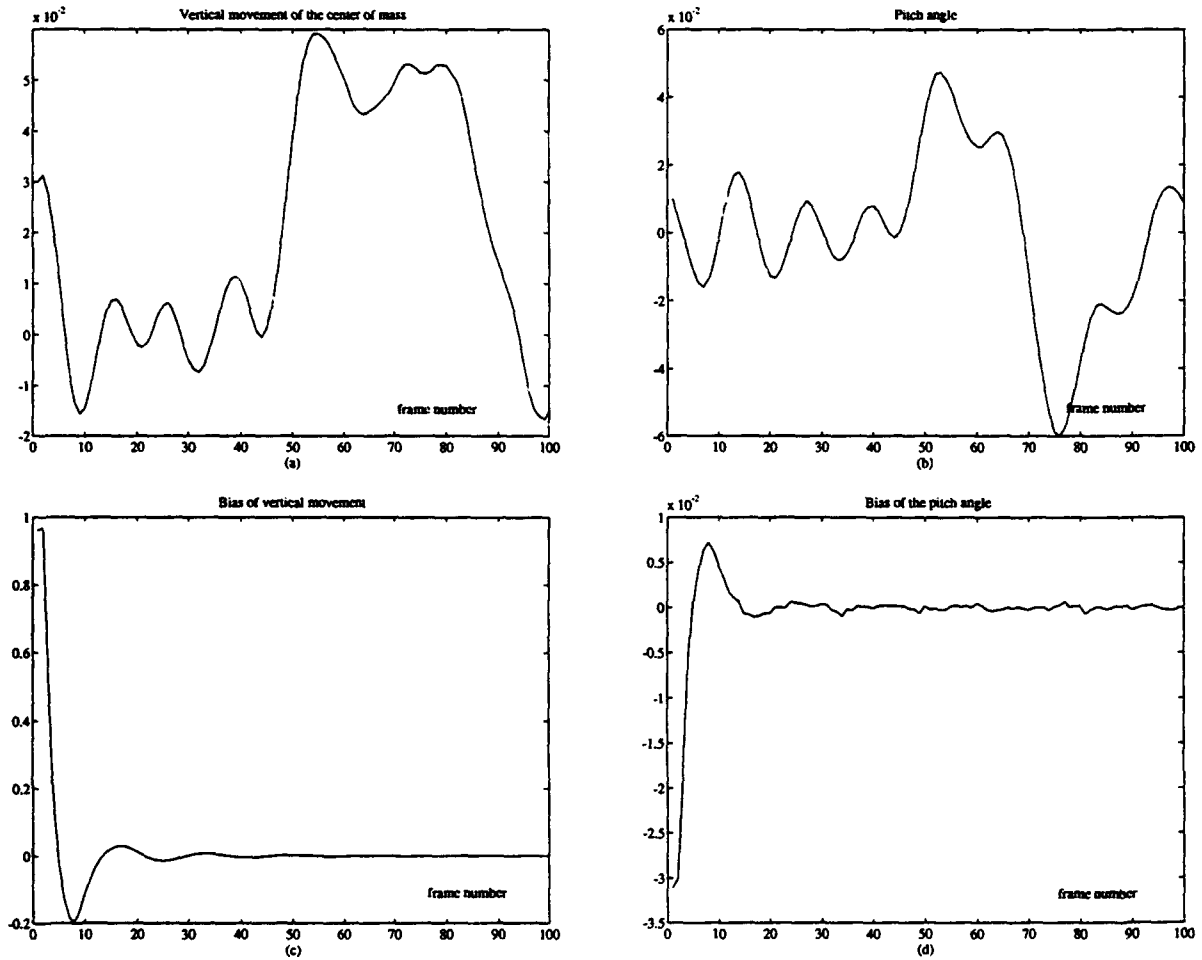


Figure 6: The time history and bias of the estimates of the motion parameters of the HVM: (a) vertical movement of the center of mass, (b) pitch angle, (c) vertical movement error, and (d) pitch angle error.

For the FVM, since the plant equation (13) is nonlinear, a numerical integration technique is employed with the initial conditions

$$(0.03 \ 1.2 \ 0.1 \ -1.5 \ -0.05 \ 1.0 \ -0.02 \ -0.9 \ 0.01 \ 0.5 \ -0.1 \ 0.2 \ 0.3 \ 0.1 \ 0.2 \ 0.8 \ 0.55678 \ 2.69)^T$$

The resulting trajectories, corresponding to the states directly related to the bouncing and orientation of the vehicle's body, are shown in Fig. 7. The nonzero instantaneous angular velocity for the FVM introduces roll motion, in addition to pitch motion, from the beginning.

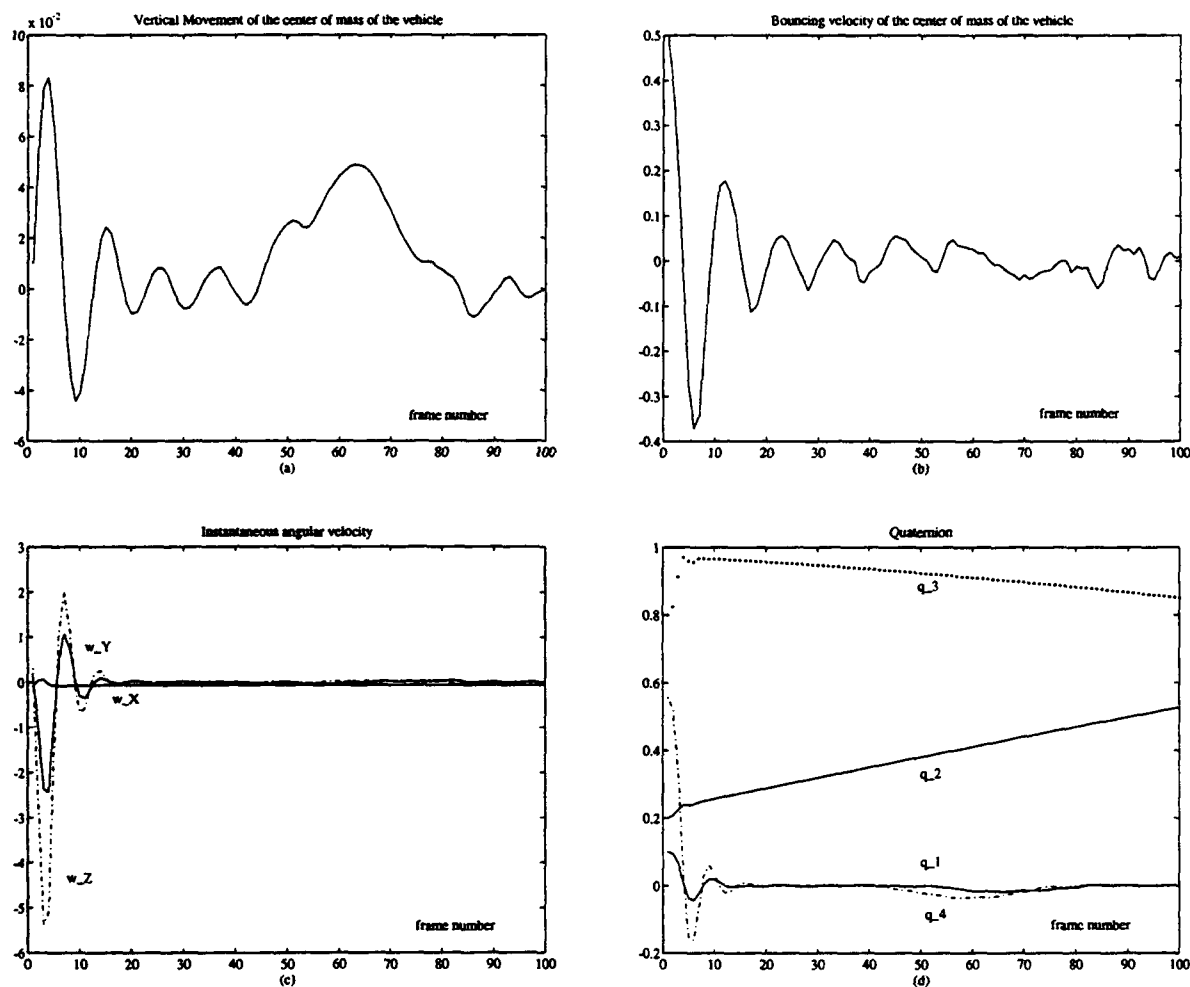


Figure 7: The time history of the motion parameters of the FVM: (a) vertical movement of the center of mass, (b) bouncing velocity, (c) instantaneous angular velocity, and (d) quaternions.

Eight feature points were used in both models. Instead of randomly generating these feature points, we used feature points from the Rocket ALV sequence, in which ground truth is available [6, 15]. Note that in this above sequence, the camera moves along a straight path toward the left. In our experiment, we shifted each point upward and to the right by 10.0 so that the corresponding

image point would be close to the center of the image. To avoid the depth becoming negative after a few frames, each point was moved away from the origin by 20.0. The resulting 3-D coordinates of the feature points in the inertial coordinate system are listed in Table 2. The size of the image is assumed to be  $2.0 \times 2.0$  with resolution  $200 \times 200$ . This is equivalent to adding 0.01 uniform noise to the image plane coordinates of each feature point. The trajectories of the feature points are then obtained from (19); the sampling rate is 10 frames/sec for both models.

Table 2: The feature point coordinates in the inertial coordinate system  $I$ .

Feature points	3-D coordinates		
1	2.317	-2.245	41.460
2	0.48	-4.894	48.559
3	1.594	-0.526	43.899
4	1.526	9.516	44.770
5	1.632	1.155	44.620
6	-0.493	-0.500	53.794
7	3.937	5.892	34.356
8	1.739	6.001	44.246

In the following, we assume that the 3-D coordinates of the feature points in the inertial coordinate system  $I$  are available. Simulations with known and unknown terrain will now be presented.

### Known Terrain

Assuming that the excitation input to each wheel is known, fifty Monte Carlo trials were done for both models. The initial guess for the recursive filter was set to be

$$(1.0 \ 1.0 \ 1.0 \ 1.0 \ 1.0 \ 1.0 \ 1.0 \ 1.0 \ 1.0)^T$$

for the HVM, and

$$(1.0 \ 1.0 \ 1.0 \ 1.0 \ 1.0 \ 1.0 \ 1.0 \ 1.0 \ 1.0 \ 1.0 \ 1.0 \ 1.0 \ 0.0 \ 0.0 \ 0.0 \ 1.0 \ 1.0)^T$$

for the FVM. Note that for the FVM, the initial guess for the quaternions should be of length 1 [16]; the initial guesses were purposely chosen to be different from the initial conditions in order to test the convergence of the IEKF. The estimates for the two models are shown in Fig. 6 and Fig. 8. As shown in these figures, the IEKF converges to the true values in about 40 frames for both models. Since the plant equation of the FVM is nonlinear, a numerical integration technique was employed in the prediction stage of the IEKF for the FVM.



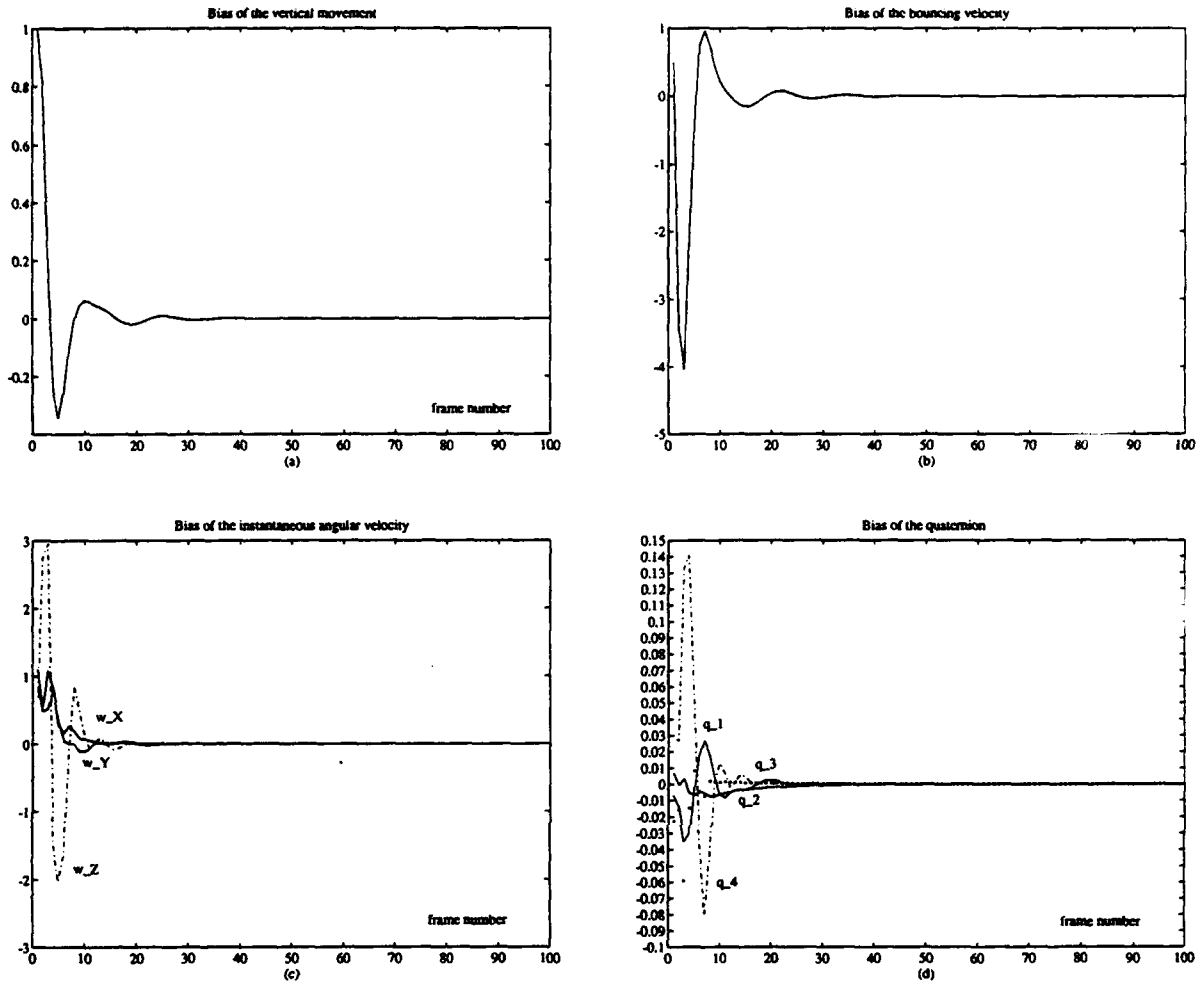


Figure 8: Bias of the estimates of the motion parameters of the FVM: (a) vertical movement error, (b) bouncing velocity error, (c) angular velocity error, and (d) quaternion error.

### Unknown Terrain

We first consider the HVM. By modeling the inputs as first order Markov processes and augmenting the state vector to include the two inputs, the plant equation (12) becomes

$$\begin{pmatrix} \dot{\underline{x}} \\ \dot{\underline{x}}_0 \end{pmatrix} = \begin{pmatrix} A & B \\ 0 & \alpha I_2 \end{pmatrix} \begin{pmatrix} \underline{x} \\ \underline{x}_0 \end{pmatrix} + \begin{pmatrix} 0 \\ I_2 \end{pmatrix} \begin{pmatrix} w_1(t) \\ w_2(t) \end{pmatrix} \quad (23)$$

where  $I_2$  is a  $2 \times 2$  identity matrix and  $\alpha$  is a constant. For simplicity,  $w_1(t)$  and  $w_2(t)$  are assumed to be independent white Gaussian noise, although correlation exists between the inputs to the front and rear wheels. Using the same measurement equations as before, the IEKF was applied, with the same initial guess as in the case of known terrain.

The estimated results are shown in Fig. 9. To illustrate the effects of measurement noise on the

IEKF, the estimates obtained when there is no measurement noise are shown in (a) and (b). The estimates with 0.001 uniform noise, corresponding to an image resolution of  $2000 \times 2000$ , are shown in (c) and (d). The state corresponding to bouncing is more sensitive to measurement noise than the pitch angle state, and the errors in the estimates are larger than those for known terrain. We have also observed that when we treat the excitation inputs as additional states, the IEKF cannot track the states corresponding to the wheel movements and inputs. In the case of known terrain, this problem did not appear. The observability of the augmented HVM (23) should be investigated.

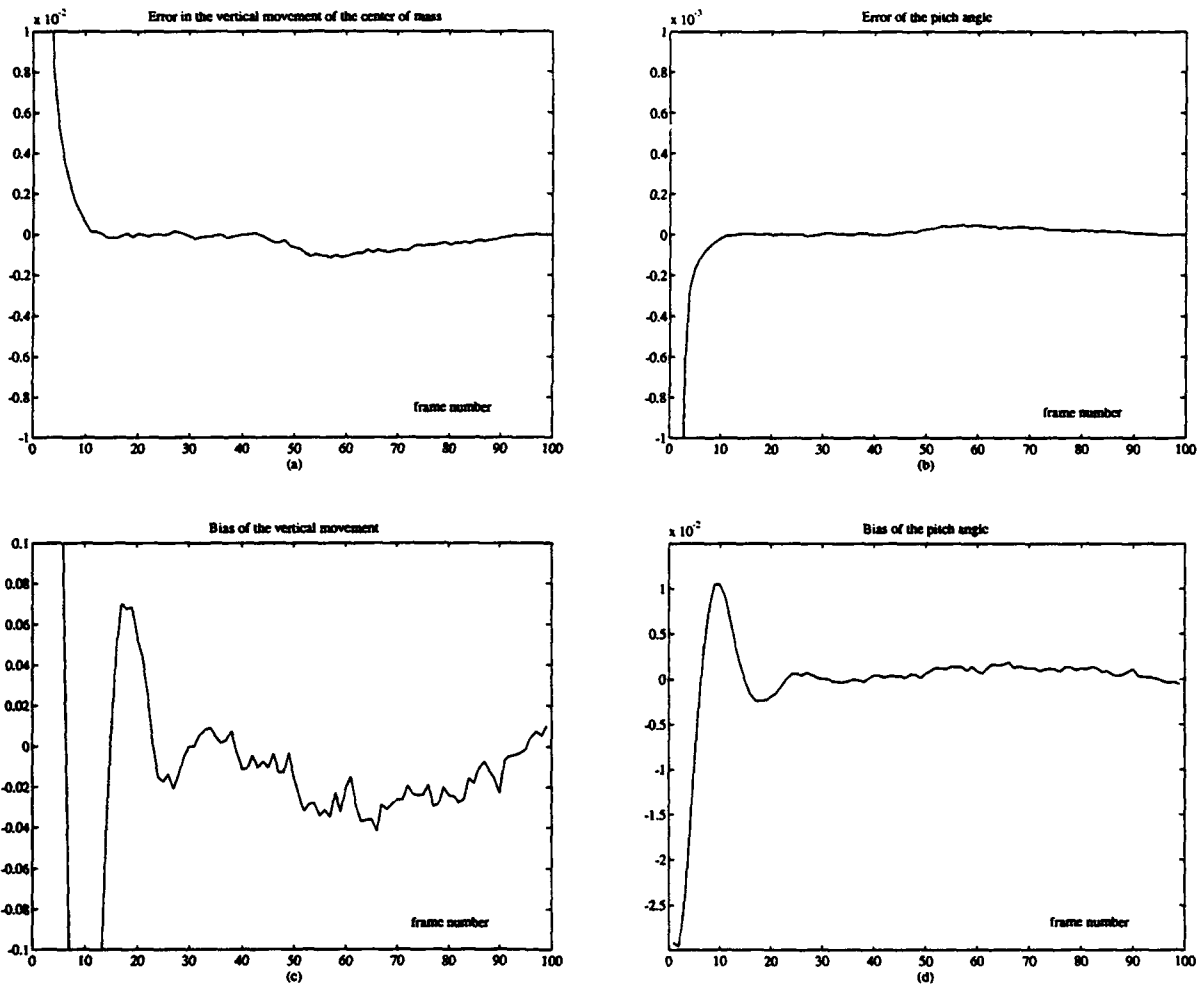


Figure 9: The effects of measurement noise on the IEKF when the excitation inputs are unknown: (a) vertical movement error without noise, (b) pitch angle error without noise, (c) vertical movement error with noise, and (d) pitch angle error with noise.

We see from the above simulation that more information seems to be required in order to obtain reliable estimates of vehicle motion when the surface inputs are not available. Such additional

information could be obtained if a Digital Terrain Model (DTM) or an active sensor such as LADAR were available. The rough estimates of the surface could then be combined with the visual inputs to provide more measurements for the IEKF. Currently we are working on this idea and plan to test it on the FVM.

## 5 Conclusion

A new algorithm has been presented for estimating the egomotion of an autonomous vehicle which navigates through uneven terrain. In this paper the vehicle is assumed to move along a straight path, but steering dynamics (or kinematics) could also be included, to take lateral motion into account. Our work can be directly applied to stabilize the images acquired during vehicle navigation. The pitch and roll angles can be estimated from the instantaneous angular velocity or from the rotation matrix for the FVM. Using knowledge of the vertical movement of the vehicle and of the pitch and roll angles, image stabilization can then be achieved.

## References

- [1] J. K. Aggarwal. Motion and time-varying imagery—An overview. In *Proc. IEEE Workshop on Motion: Representation and Analysis*, pages 1–6, Kiawah Island, SC, May 1986.
- [2] J. K. Aggarwal and A. Mitiche. Structure and motion from images: Fact and fiction. In *Proc. Third Workshop on Computer Vision: Representation and Control*, pages 127–128, Bellaire, MI, October 1985.
- [3] T. J. Broida and R. Chellappa. Estimating the kinematics and structure of a rigid object from a sequence of monocular images. *IEEE Trans. Patt. Anal. Mach. Intell.*, PAMI-13:497–513, June 1991.
- [4] M. Demić. Optimisation of the characteristics of the elasto-damping elements of a passenger car by means of a modified Nelder-Mead method. *Int. J. Vehicle Design*, 10:136–152, 1989.
- [5] E. D. Dickmanns and B. D. Mysliwetz. Recursive 3-D road and relative ego-state recognition. *IEEE Trans. Patt. Anal. Mach. Intell.*, PAMI-14:199–213, February 1992.
- [6] R. Dutta et al. A data set for quantitative motion analysis. In *Proc. IEEE Conf. on Computer Vision and Pattern Recognition*, pages 159–164, San Diego, CA, June 1989.

- [7] J. Q. Fang and T. S. Huang. Some experiments on estimating the 3-D motion parameters of a rigid body from two consecutive image frames. *IEEE Trans. Patt. Anal. Mach. Intell.*, PAMI-6:545-554, September 1984.
- [8] A. Hady and D. A. Crolla. Theoretical analysis of active suspension performance using a four-wheel vehicle model. *Proc. Inst. Mech. Engrs*, 203:125-135, 1989.
- [9] B. K. P. Horn. *Robot Vision*. M. I. T. Press, Cambridge, MA, 1986.
- [10] T. S. Huang. Motion detection and estimation from stereo image sequences: Some preliminary experimental results. In *Proc. IEEE Workshop on Motion: Representation and Analysis*, pages 45-46, Kiawah Island, SC, May 1986.
- [11] P. S. Maybeck, ed. *Stochastic Models, Estimation, and Control*, volume 2. Academic Press, New York, 1982.
- [12] I. H. Shames. *Engineering Mechanics, Volume II, Dynamics*. Prentice-Hall, Englewood Cliffs, NJ, 1980.
- [13] C. E. Thorpe, ed. *Vision and Navigation*. Kluwer Academic, Boston, 1990.
- [14] J. Weng, T. S. Huang, and N. Ahuja. 3-D motion estimation, understanding, and prediction from noisy image sequences. *IEEE Trans. Patt. Anal. Mach. Intell.*, PAMI-9:370-389, May 1987.
- [15] T. H. Wu and R. Chellappa. 3-D recovery of structural and kinematic parameters from a long sequence of noisy images. In *Proc. Image Understanding Workshop*, pages 641-651, Washington, DC, April 1993.
- [16] G. S. Young and R. Chellappa. 3-D motion estimation using a sequence of noisy stereo images: Models, estimation, and uniqueness results. *IEEE Trans. Patt. Anal. Mach. Intell.*, PAMI-12:735-759, August 1990.

## Appendix A

To apply Euler's equations of motion as stated in Section 3, we need to express  $(M_x, M_y, M_z)^T$  in terms of the state vector  $\underline{x}$ .

Consider Fig. 3 and assume that  $\{\vec{F}_i, i = 1, \dots, 4\}$  always act along the  $\vec{i}$ -direction, i.e.  $\vec{F}_i$  in  $I = (F_{iX}, 0, 0)^T$ ; then

$$\vec{F}_i \text{ in } V \equiv (F_{ix}, F_{iy}, F_{iz})^T \quad (24)$$

$$= (r_1 \ r_2 \ r_3)^T F_{iX} \quad (25)$$

where  $(r_1 \ r_2 \ r_3)$  is the first row of the rotation matrix  $R[q]$  in (10).

Let the position vectors of the four corners of the vehicle's body with respect to coordinate system  $V$  be  $\{\vec{r}_i, i = 1, \dots, 4\}$ , i.e.

$$\vec{r}_1 = (0, T_s, W_A)^T \quad \vec{r}_2 = (0, -T_s, W_A)^T$$

$$\vec{r}_3 = (0, T_s, -W_B)^T \quad \vec{r}_4 = (0, -T_s, -W_B)^T$$

The net torque applied by the four forces can then be obtained as follows:

$$\begin{aligned} \begin{pmatrix} M_x \\ M_y \\ M_z \end{pmatrix} &= \sum_{i=1}^4 \vec{r}_i \times \vec{F}_i \text{ in } V \quad (26) \\ &= \begin{pmatrix} r_3 T_s - r_2 W_A & -r_3 T_s - r_2 W_A & r_3 T_s + r_2 W_B & -r_3 T_s + r_2 W_B \\ r_1 W_A & r_1 W_A & -r_1 W_B & -r_1 W_B \\ -r_1 T_s & r_1 T_s & -r_1 T_s & r_1 T_s \end{pmatrix} \begin{pmatrix} F_{1X} \\ F_{2X} \\ F_{3X} \\ F_{4X} \end{pmatrix} \end{aligned}$$

Substitution of (5) and (15) into (26) yields the desired relationship between  $(M_x, M_y, M_z)^T$  and  $\underline{x}$ .

REPORT DOCUMENTATION PAGE			Form Approved OMB No. 0704-0188	
<small>Public reporting burden for this collection of information is estimated to average 1 hour per response, including the time for reviewing instructions, searching existing data sources, gathering and maintaining the data needed, and completing and reviewing the collection of information. Send comments regarding this burden estimate or any other aspect of this collection of information, including suggestions for reducing this burden, to Washington Headquarters Services, Directorate for Information Operations and Reports, 1215 Jefferson Davis Highway, Suite 1204, Arlington, VA 22202-4302, and to the Office of Management and Budget, Paperwork Reduction Project (0704-0188), Washington, DC 20503.</small>				
1. AGENCY USE ONLY (Leave blank)	2. REPORT DATE NOVEMBER 1993	3. REPORT TYPE AND DATES COVERED TECHNICAL		
4. TITLE AND SUBTITLE ESTIMATION OF VEHICLE DYNAMICS FROM MONOCULAR NOISY IMAGES		5. FUNDING NUMBERS		
6. AUTHOR(S) Yi-Sheng Yao and Rama Chellappa		DA AHO4-93G-0419		
7. PERFORMING ORGANIZATION NAME(S) AND ADDRESS(ES) Center for Automation Research University of Maryland College Park, MD 20742-3275		8. PERFORMING ORGANIZATION REPORT NUMBER CSR-TR-692 CS-TR-3172		
9. SPONSORING/MONITORING AGENCY NAME(S) AND ADDRESS(ES) U.S. Army Research Office P.O. Box 12211 Research Triangle Park, NC 27709-2211		10. SPONSORING/MONITORING AGENCY REPORT NUMBER ARO 32365.1-MA		
11. SUPPLEMENTARY NOTES The views, opinions and/or findings contained in this report are those of the author(s) and should not be construed as an official Department of the Army position, policy, or decision, unless so designated by other documentation.				
12a. DISTRIBUTION/AVAILABILITY STATEMENT Approved for public release; distribution unlimited.		12b. DISTRIBUTION CODE		
13. ABSTRACT (Maximum 200 words) This paper presents a new model-based egomotion estimation algorithm for an autonomous vehicle navigating through rough terrain. Due to the uneven terrain, the vehicle undergoes bouncing, pitch and roll motion. To reliably accomplish other tasks such as tracking and obstacle avoidance using visual inputs, it is essential to consider these disturbances. In this paper, two vehicle models available in the literature are used for egomotion estimation. The Half Vehicle Model (HVM) takes into account the bouncing and pitch motion of the vehicle, and the Full Vehicle Model (FVM) also considers the roll motion. The dynamics of the vehicle are formulated using standard equations of motion. Assuming that depth information is known for some landmarks in the scene (e.g., obtained from a laser range finder), a feature-based approach is proposed to estimate vehicle motion parameters such as the vertical movement of the center of mass and the instantaneous angular velocity. An Iterated Extended Kalman Filter (IEKF) is used for recursive parameter estimation. Simulation results for both known and unknown terrain are presented.				
14. SUBJECT TERMS Motion estimation, navigation, vehicle dynamics		15. NUMBER OF PAGES 24		
		16. PRICE CODE		
17. SECURITY CLASSIFICATION OF REPORT UNCLASSIFIED	18. SECURITY CLASSIFICATION OF THIS PAGE UNCLASSIFIED	19. SECURITY CLASSIFICATION OF ABSTRACT UNCLASSIFIED	20. LIMITATION OF ABSTRACT UL	